

Analysis of Age of Information in Non-terrestrial Networks

Yanwu Lu[†], Howard H. Yang[†], Nikolaos Pappas[‡], Giovanni Geraci^{*}, Chuan Ma[§], and Tony Q. S. Quek[¶]

[†]ZJU-UIUC Institute, Zhejiang University, Haining, China

[‡]Department of Computer and Information Science, Linköping University, Linköping, Sweden

^{*}Telefonica Research and Universitat Pompeu Fabra, Barcelona, Spain

[§]Zhejiang Lab, Hangzhou, China

[¶]Information System and Technology Design Pillar, Singapore University of Technology and Design, Singapore

Abstract—Non-terrestrial networks (NTN), particularly low Earth orbit (LEO) satellite networks, have emerged as a promising solution to overcome the limitations of traditional terrestrial networks in the context of next-generation (6G) wireless systems. In this paper, we focus on analyzing the timeliness of information delivery in NTN through the concept of Age of Information (AoI). We propose an on-off process to approximate the service process between LEO satellites and a source node located on the Earth’s surface. By utilizing stochastic geometry, we derive a closed-form expression for the time-average AoI in an NTN. This expression also applies to on-off processes with one component following an exponential distribution while the other has its probability density function supported on a bounded interval. Numerical results validate the accuracy of our analysis and demonstrate the impact of source status update rate and satellite constellation density on the time-average AoI. Our work fills a gap in the literature by providing a comprehensive analysis of AoI in NTN and offers new insights into the performance of LEO satellite networks.

I. INTRODUCTION

Non-terrestrial networks (NTN) have emerged as a potential technological breakthrough in the realm of wireless systems, particularly in the context of next-generation (6G) networks [1]–[5]. NTN offer a promising solution to overcome the limitations of traditional terrestrial networks [6]–[8]. Mega satellite constellation design and standardization efforts are currently underway [9], [10], showcasing the growing interest in this field. Among NTN platforms, low Earth orbit (LEO) satellites have gained significant attention due to their advantages of relatively low latency and operating cost [11], [12]. Numerous LEO satellites have already been deployed at various orbits to provide global commercial communication services [13]. However, as the number of deployed LEO satellites increases, the performance of the network, particularly the timeliness of information delivery, requires careful investigation.

In order to assess the timeliness of information successfully received in an NTN, the concept of *Age of Information* (AoI) may serve as an appropriate metric [14], [15]. AoI provides insights into the freshness of information by measuring the time elapsed since the generation of the most recent update at a particular destination [16]. By analyzing the mean AoI, it may become possible to estimate the delivery performance of

the entire network [17]. It is worth noting that LEO satellites operate at extremely fast speeds in orbit, resulting in frequent transitions between connected and disconnected states. These transitions inevitably lead to an increase in AoI.

To analyze the performance of NTN, researchers have employed stochastic geometry as a mathematical tool, enabling the modeling of satellite locations and the derivation of expressions for coverage probability [18]. For instance, previous studies have modeled the location of LEO satellites using a binomial point process (BPP) on a sphere [19]. Other works have considered systems of multiple concentric spheres, with satellites uniformly distributed as BPP on each sphere [20]. Analytic formulations for coverage probability in dense satellite constellations have also been proposed [21], [22].

While these existing works have individually addressed certain aspects of NTN, there remains a gap in the literature when it comes to analyzing the AoI in such networks. Specifically, owing to the various positions of satellites and their communication capabilities, the connected (and disconnected) periods of the satellite links are strongly affected by network configurations. The AoI performance has not yet been well understood in this scenario. In this article, we aim to fill this gap by studying the AoI in a LEO satellite network. We consider a system where satellite positions follow a Poisson point process (PPP) and model the satellite service process as an on-off process, where updates arriving during the off-service period are dropped. The recent study [23] has analyzed AoI under an on-off process, and is closely related to our work. However, the analysis in [23] was limited to the case of on and off periods being exponentially distributed, which, is unable to express satellite service process in this paper. Our main contributions can be summarized as follows:

- We formulate, for the first time, the notion of AoI in an NTN. We do so by establishing an on-off process that approximates the service process between orbiting LEO satellites and a source node located on the Earth.
- Through stochastic geometry tools, we derive a closed-form expression for the time-average AoI in an NTN. This result also extends the AoI analysis under on-off processes [23] into scenarios where one component

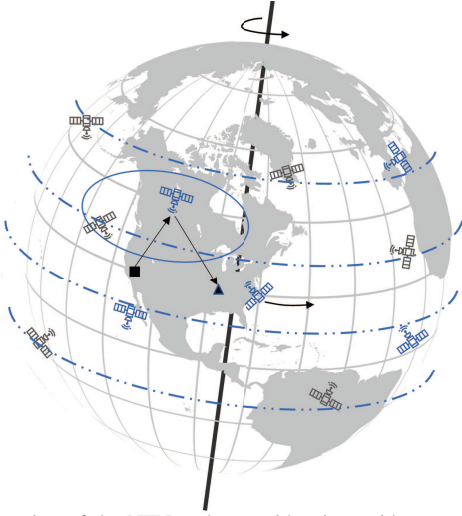


Fig. 1. Illustration of the NTN under consideration, with a constellation of LEO satellites deployed on a sphere and connecting source-destination nodes.

follows an exponential distribution while the other has its probability density function supported on a bounded interval.

- We provide numerical results that validate the accuracy of our analysis and quantify the impact of both the source status update rate and the satellite constellation density on the time-average AoI.

II. SYSTEM MODEL

In this section, we introduce the network topology under consideration, the traffic generation and propagation channel models, and the performance metric of our analysis.

Network topology: We consider an NTN consisting of a constellation of LEO satellites deployed at the same altitude h . We assume the positions of the satellites to follow a homogeneous Poisson point process (PPP) [21], [24], [25] of intensity λ on a sphere of radius $R_{\oplus} + h$, where $R_{\oplus} = 6371$ km denotes the Earth radius. We focus on a source node on the ground that updates its latest status to a destination node. We consider the scenario where the source and destination are both out of the coverage of a terrestrial network. Hence, communication needs to take place via an NTN, through satellite nodes. An illustrative example of this setup is provided in Fig. 1.

Traffic generation and propagation channel: We assume the source node to employ a *generate-at-will* approach [15] for status updates, where a packet is transmitted immediately after its generation. Specifically, we consider the interval between the generation of two consecutive status updates to be independently and identically distributed (i.i.d.), following an exponential distribution with rate μ . We further assume the source node to send out information packets at a fixed transmit power P_{tx} , where the signal propagation is subject to path loss that obeys power law with path loss exponent α , and reception experiences white Gaussian noise with variance σ^2 .

Coverage and information delivery: We deem a source node to be covered by a satellite when its signal-to-noise ratio (SNR) surpasses a minimum decoding threshold θ . Out of the

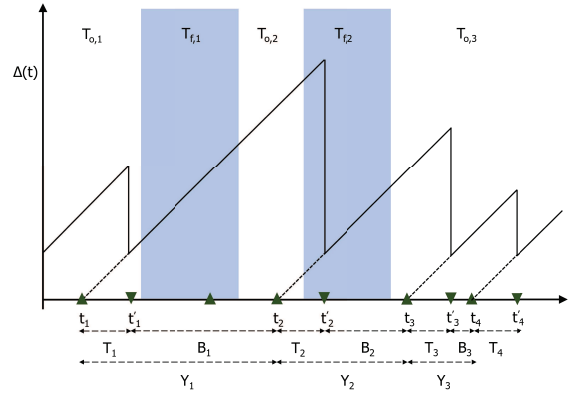


Fig. 2. Example of AoI evolution under on- and off-service periods, which is relevant to intermittent NTN connectivity.

satellites from which it receives coverage, the source node then connects to at most one, namely the one providing the largest received power. If the source node is connected to a satellite upon generating a new status update, the corresponding information packet can be successfully delivered to the destination after experiencing a constant propagation delay D .¹ However, owing to the mobility nature of satellites, any satellite providing coverage eventually moves away from the source node, being replaced by a new satellite. Before the arrival of another satellite, the source node will remain out of coverage, with any status updates generated during this period being undelivered.

Key performance indicator: In this paper, we study the AoI in an NTN. AoI quantifies the *freshness* of the information received at a destination node, and it is formally defined as follows:

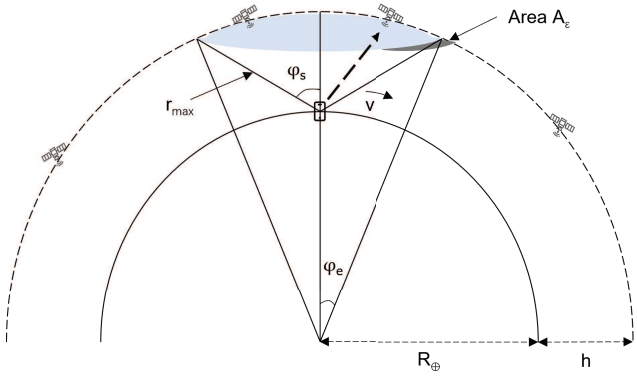
$$\Delta(t) = t - G(t), \quad (1)$$

where $G(t)$ is the timestamp at which the latest update received by the destination at time slot t was generated at the source. The inherent dynamics of the NTN cause the availability of satellite connectivity to be intermittent. Therefore, updates from the source node can only be successfully delivered while such connectivity is available. As a result, the evolution of the AoI in an NTN follows a trajectory as per Fig. 2, where shaded areas correspond to intervals of lack of connectivity, during which any newly generated updates are lost. To capture the overall timeliness in the delivery of status updates through an NTN, we then define the time-average AoI as follows:

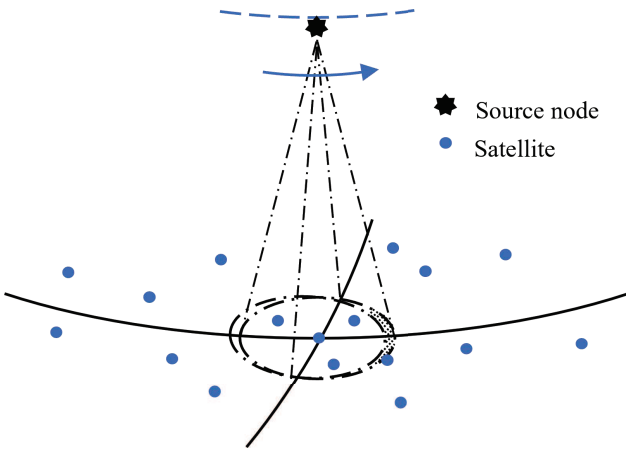
$$\bar{\Delta} = \lim_{T \rightarrow \infty} \frac{1}{T} \int_0^T \Delta(t) dt. \quad (2)$$

In the next section, we derive an expression for $\bar{\Delta}$ in the NTN under consideration, and we shed light on how it is affected by the key NTN system-level parameters.

¹We assume the transmission from a satellite to the destination node to be always available. We focus on the uplink transmission from the source node to a satellite as this typically represents the bottleneck due to a limited transmission power budget.



(a) Side view of the NTN, with a shaded area containing satellites whose distance from the source node is smaller than r_{\max} .



(b) NTN as seen from the standpoint of the source node, with a shaded area indicating the relative movement of the satellites with respect to the source node.

Fig. 3. Illustration of the relative motion between a source node and satellites.

III. ANALYSIS OF AOI IN NTN

We begin by characterizing the distribution of the intervals during which the source node is connected/disconnected to/from the NTN, which we denote as the *on-* and *off-service* periods. We then derive the analytical expression for the time-average AoI and discuss special cases to provide additional insights.

A. Distribution of the On-Off Service Periods

At time t , let $r(t)$ denote the distance between the source node and the closest satellite. Then the corresponding SNR can be expressed as

$$\text{SNR}(t) = \frac{P_{\text{tx}} r(t)^{-\alpha}}{\sigma^2}. \quad (3)$$

Since the source node can reliably connect to the satellite only when the SNR surpasses a minimum decoding threshold, i.e., $\text{SNR}(t) > \theta$, equation (3) yields a maximum transmission distance for successful decoding, $r_{\max} = (P_{\text{tx}}/\sigma^2\theta)^{\frac{1}{\alpha}}$. From the perspective of the source node, the maximum transmission

distance separates the sphere over which the satellites are located into two parts, as depicted in Fig. 3(a): (i) a shaded area, corresponding to a dome in the sphere, whereby any satellite has a distance from the source node that is smaller than r_{\max} and can thus establish a connection; (ii) the remaining area, containing satellites that are too far from the source node to provide connectivity. As illustrated in Fig. 3(a), the distance r_{\max} is related to the node-centered zenith angle φ_s and the Earth-centered zenith angle φ_e . More precisely, r_{\max} can be expressed as a function of φ_e and φ_s as follows

$$r_{\max} = \frac{(R_{\oplus} + h) \cos(\varphi_e) - R_{\oplus}}{\cos(\varphi_s)}, \quad (4)$$

where φ_e is related to φ_s as

$$\varphi_e = \cot^{-1} \left(\frac{\cot(\varphi_s) + \rho \sqrt{\cot^2(\varphi_s) + 1 - \rho^2}}{1 - \rho^2} \right), \quad (5)$$

in which $\rho = R_{\oplus}/(R_{\oplus} + h)$.

As shown in Fig. 3(a), each satellite lying in the shaded dome region has a relative velocity with respect to the source node owed to its orbital movement and the Earth's rotation. Such relative speed causes the satellite to rapidly pass through the shaded region. In what follows, we focus on the satellites within the dome region and their motion mode. While there are multiple satellite orbits, the maximum arc length within the specific dome region remains fixed. We assume that the velocity difference between the satellites and the source node remains constant. By considering relative motion, we can treat all satellites within the dome region as stationary in space, similar to stars in the sky that appear static for a short period of time. Meanwhile, the source node undergoes circular movements at a velocity v . Furthermore, we assume that after completing a full cycle, the positions of the satellites are regenerated independently, following a homogeneous PPP with a density of λ .

The duration for which a satellite remains within the dome region can be approximated as an on-service period, while the time between a satellite's departure from the dome region and the arrival of the subsequent satellite can be viewed as an off-service period. Due to the random positions of the satellites, the durations of both the on- and off-service periods vary. However, we can approximate these periods as independently and identically distributed. In the subsequent analysis, we leverage the techniques developed in [26] to derive the distributions of the on- and off-service periods, taking into account the aforementioned approximations.

Theorem 1: *The off-service periods follow an identical exponential distribution with density given by*

$$\lambda_{\text{os}} = 2\omega\lambda \sin(\varphi_e) (R_{\oplus} + h)^2 \quad (6)$$

where $\omega = v/R_{\oplus}$ and the on-service periods have a common probability density function (PDF) given as

$$f_W(s) = \begin{cases} \frac{\omega \cos(\varphi_e) \tan(\frac{\omega s}{2})}{2\varphi_e \sqrt{\sin^2(\varphi_e) - \sin^2(\frac{\omega s}{2})}}, & \text{if } s \in [0, \frac{2\varphi_e}{\omega}], \\ 0, & \text{otherwise.} \end{cases} \quad (7)$$

Proof: Note that the dome area changes as the source node moves. Since the satellites are scattered as a PPP with intensity λ , for a small value of time duration ϵ , the number of satellites arriving for each period of duration ϵ is λA_ϵ , where

$$A_\epsilon = 2(R_\oplus + h)^2 \omega \epsilon \sin(\varphi_e) \quad (8)$$

is the area of the dome moving in the interval ϵ as shown in Fig. 3(b). This implies that (a) the increments in the satellite arrival process have the same distribution (because (8) holds irrespective of the source node's position) and (b) the number of satellites in any two disjoint areas are independent. As such, we can conclude that the off-service periods are exponentially distributed with the rate $2\omega\lambda\sin(\varphi_e)(R_\oplus + h)^2$.

On the other hand, the trajectory of each satellite in the dome section is characterized by the latitude difference between the source node and the point of the satellite projected on the ground, where these together determine the total service time of each satellite when establishing a connection with the source node. Let Θ denote the angle difference that represents the possible entry location of satellites, following a uniform distribution on $[-\varphi_e, \varphi_e]$. The service time W is thus a random variable given by

$$W = \frac{2}{\omega} \arcsin \left(\frac{\sqrt{\sin^2(\varphi_e) - \sin^2(\Theta)}}{\cos(\Theta)} \right). \quad (9)$$

The PDF of W can then be derived using the distribution of Θ . \square

B. Analytical Expression of the AoI in NTN

As illustrated in Fig. 2, we use t_k and t'_k to represent the timestamps corresponding to the transmit and receive instances of the k -th update. We denote by $T_{o,i}$ and $T_{f,i}$ the duration of the i -th on- and off-service periods, respectively. If the k -th packet transmission is successful, $T_k = t'_k - t_k = D$ denotes the propagation delay and $Y_k = T_k + B_k$ indicates the period between the k -th and $k+1$ -th received updates, where $B_k = t_{k+1} - t'_k$. Following [23], the time-average AoI can be expressed as

$$\bar{\Delta} = \frac{\mathbb{E}[Y_k^2] + 2\mathbb{E}[T_k Y_k]}{2\mathbb{E}[Y_k]} = \frac{\mathbb{E}[Y_k^2]}{2\mathbb{E}[Y_k]} + D. \quad (10)$$

Since the AoI evolves across a series of on- and off-service periods, calculating the expectations in (10) entails determining two conditional probabilities: (a) the probability that the next update is generated during an on-service period, given that the latest update occurred in an on-service period, and (b) the probability that the next update will be generated in an off-service period if the latest update occurred during an off-service period. We denote these probabilities as $P_{o|o}$ and $P_{f|f}$, respectively, and we characterize them in the following lemma.

Lemma 1: *The conditional probability $P_{f|f}$ is given by*

$$P_{f|f} = \frac{1-a}{1-ab}, \quad (11)$$

where $a = \lambda_{os}/(\mu + \lambda_{os})$ and $b = \int_{-\infty}^{\infty} e^{-\mu s} f_W(s) ds$. The conditional probability $P_{o|o}$ is

$$P_{o|o} = \frac{1 - (2 - P_{f|f}) P_{off}}{1 - P_{off}}, \quad (12)$$

where $P_{off} = 1/(1 + \lambda_{os} \mathbb{E}[W])$.

Proof: Without loss of generality, we assume an update is generated in the first off period at $t = 0$. We use s'_i and s_i to represent the start times of the i -th on- and off-service periods, respectively. As each on- and off-service period is distinct and non-overlapping, the probability of the next update remaining in an off-service period is obtained by adding up the probabilities of arrival within each individual off-service period:

$$\begin{aligned} P_{f|f}^{Cond} &= \sum_{i=1}^{\infty} [F(s'_i) - F(s_i)], \\ &= \sum_{i=1}^{\infty} [\exp(-\mu s_i) - \exp(-\mu(s_i + T_{f,i}))], \\ &= \sum_{i=1}^{\infty} [1 - \exp(-\mu T_{f,i})] \prod_{k=1}^{i-1} \exp(-\mu(T_{f,k} + T_{o,k})). \end{aligned} \quad (13)$$

By deconditioning random variables $\{T_{o,i}\}_{i \geq 1}$ and $\{T_{f,i}\}_{i \geq 1}$ in the above (and notice that they are i.i.d.), we have

$$\begin{aligned} P_{f|f} &= \sum_{i=1}^{\infty} \mathbb{E}_{T_f} [1 - e^{-\mu T_f}] (\mathbb{E}_{T_f} [e^{-\mu T_o}] \mathbb{E}_{T_o} [e^{-\mu T_f}])^{i-1} \\ &= \left(1 - \frac{\lambda_{os}}{\mu + \lambda_{os}}\right) \sum_{l=0}^{\infty} \left(\frac{\lambda_{os}}{\mu + \lambda_{os}} \int e^{-\mu s} f_W(s) ds\right)^l \\ &= \frac{1 - \frac{\lambda_{os}}{\mu + \lambda_{os}}}{1 - \frac{\lambda_{os}}{\mu + \lambda_{os}} \int e^{-\mu s} f_W(s) ds}. \end{aligned} \quad (14)$$

Let P_{off} denote the probability that a random point is in an off-service period. We have that

$$P_{off} = \frac{\sum_{l=0}^{\infty} \mathbb{E}[T_{f,l}]}{\sum_{l=0}^{\infty} (\mathbb{E}[T_{f,l}] + \mathbb{E}[T_{o,l}])} = \frac{1}{1 + \lambda_o \mathbb{E}[W]} \quad (15)$$

Let P_{ff} denote the probability that two adjacent updates are generated in one or different off-service periods and P_{fo} denote the probability that two adjacent updates that the previous is generated in an off-service period and the latter is generated in an on-service period. Similarly, we denote the probabilities of the other two cases as P_{oo} and P_{of} . We obtain $P_{ff} = P_{f|f} P_{off}$ and $P_{fo} = (1 - P_{f|f}) P_{off}$. Since $P_{fo} = P_{of}$, we have that

$$P_{oo} = 1 - P_{of} - P_{fo} - P_{ff} = 1 - (2 - P_{f|f}) P_{off} \quad (16)$$

and obtain

$$P_{o|o} = \frac{P_{oo}}{1 - P_{off}}. \quad (17)$$

\square

Using the results in Lemma 1, we can compute the first and second moments of Y_k as follows.

Lemma 2: *The first and second moments of Y_k are given by*

$$\mathbb{E}[Y_k] = \frac{1}{\mu} + \frac{\gamma}{\mu} (1 - P_{o|o}), \quad (18)$$

and

$$\mathbb{E}[Y_k^2] = \frac{2}{\mu^2} + \frac{2(\gamma + \gamma^2)}{\mu^2} (1 - P_{o|o}), \quad (19)$$

where $\gamma = 1/(1 - P_{f|f})$.

Proof: Let Z represent the interval time between two consecutive arrivals of status updates. Each update encounters one of the situations: (a) being accepted during the on-service period, or (b) being dropped during the off-service period. After a delivery failure, the AoI keeps increasing until a new arrival falls within the on-service period. By assuming that the subsequent arrival occurs during the on-service period when the previous one is accepted, we can easily derive

$$\mathbb{E}[Y_k^o] = \mathbb{E}[Z] = \frac{1}{\mu}. \quad (20)$$

Similarly, we obtain that

$$\begin{aligned} \mathbb{E}[Y_k^f] &= \sum_{n=2}^{\infty} \left[\sum_{l=1}^n \mathbb{E}[Z_l] \right] P_{f|f}^{n-2} (1 - P_{f|f}), \\ &= \frac{1}{\mu} \left(1 + \frac{1}{1 - P_{f|f}} \right). \end{aligned} \quad (21)$$

The mean of Y_k is thus given by

$$\mathbb{E}[Y_k] = \mathbb{E}[Y_k^o] P_{o|o} + \mathbb{E}[Y_k^f] (1 - P_{o|o}). \quad (22)$$

Further, we can obtain the two terms forming the second moment of Y_k respectively as

$$\mathbb{E}[Y_k^{2,o}] = \mathbb{E}[Z^2] = \frac{2}{\mu^2} \quad (23)$$

and

$$\mathbb{E}[Y_k^{2,f}] = \sum_{n=2}^{\infty} \left[\left(\sum_{l=1}^n \mathbb{E}[Z_l] \right)^2 \right] P_{f|f}^{n-2} (1 - P_{f|f}). \quad (24)$$

Since Z_l follows exponential distribution with parameter μ , we have $S_n = \sum_{l=1}^n Z_l \sim \Gamma(n, \mu^{-1})$ and we obtain

$$\begin{aligned} \mathbb{E}[Y_k^{2,f}] &= \sum_{n=2}^{\infty} \left[\frac{n(n+1)}{\mu^2} \right] P_{f|f}^{n-2} (1 - P_{f|f}), \\ &= \frac{2 P_{f|f}^2 - 3 P_{f|f} + 3}{\lambda^2 (1 - P_{f|f})^2}. \end{aligned} \quad (25)$$

The second moment of Y_k thus yields

$$\mathbb{E}[Y_k^2] = \mathbb{E}[Y_k^{2,o}] P_{o|o} + \mathbb{E}[Y_k^{2,f}] (1 - P_{o|o}). \quad (26)$$

□

Using the above lemmas, we can obtain the analytical expression of the time average AoI.

Theorem 2: *The time-average AoI of the source-destination link in the considered system is*

$$\bar{\Delta} = \frac{\gamma^2(1 - P_{o|o})}{\mu + \mu\gamma(1 - P_{o|o})} + \frac{1}{\mu} + D. \quad (27)$$

Proof: Equation (27) is obtained by substituting $\mathbb{E}[Y_k]$ and $\mathbb{E}[Y_k^2]$ from Lemma 2 into (10). □

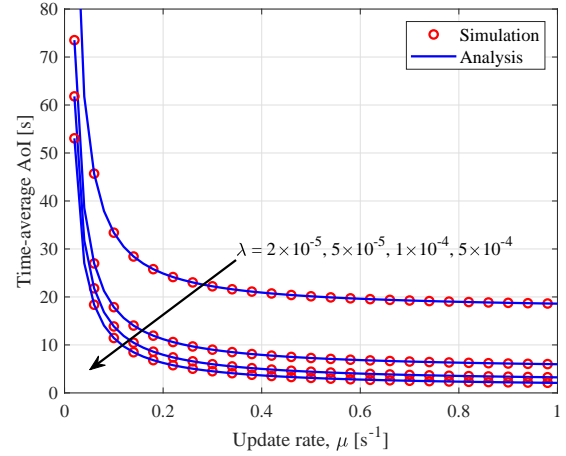


Fig. 4. Time-average AoI versus the status update rate under constellation densities λ ranging from 2×10^{-5} to $5 \times 10^{-4} \text{ km}^{-2}$, corresponding to 12924 and 323100 satellites deployed in the spherical surface, respectively.

IV. VALIDATION AND CASE STUDIES

In this section, we validate the accuracy of our analysis and evaluate the time-average AoI under different NTN scenarios. For ease of notation, we employ the Earth-centered zenith angle φ_s , rather than r_{\max} , to represent the source node dome area. Unless otherwise specified, we use the following parameters: $h = 800 \text{ km}$, $\omega = \pi/3600 \text{ rad/s}$, $\varphi_s = 1^\circ$, and $D = 1 \text{ s}$.

We evaluate the time-average AoI under a varying number of satellites in the constellation and for different status update arrival rates. Specifically, we deploy the satellite nodes on the sphere according to a homogeneous PPP. The source node cycles under velocity $v = \omega R_\oplus$. Every time upon finishing a complete circle, we regenerate the positions of all satellites using the same distribution. We run each simulation with 10^6 arrivals and collect the corresponding AoI statistics to calculate the average.

Fig. 4 shows the time-average AoI as a function of the source node status update rate, for different values of the total number of satellites passing the dome region in the constellation ranging from 225 to 5638.² This figure shows a close match between the numerical results and our theoretical analysis, thus verifying the accuracy of Theorem 2. Additionally, Fig. 4 shows that as deployment density increases, the rate of the time-average AoI descent gradually decreases. This is because the mean off-service period becomes smaller and the proportion of the on-service period becomes larger. It makes arrivals more probability get into the on-service period and be close to the value of $1/\mu$.

Fig. 5 shows the time-average AoI as a function of the node-centered zenith angle. We note that the duration of the on-service periods increases as the node-centered zenith angle becomes larger. This causes the arrivals to have a higher

²As a reference, at the time of writing Starlink and OneWeb constellations respectively consist of about 4,000 and 500 LEO satellites [27]–[29].

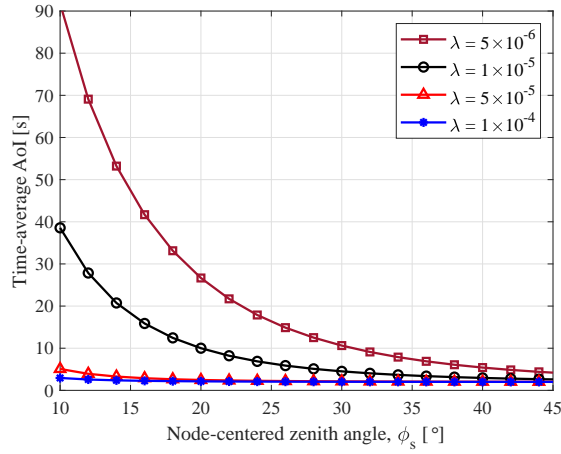


Fig. 5. Time-average AoI versus the node-centered zenith angle under constellation densities λ ranging from 5×10^{-6} to $1 \times 10^{-4} \text{ km}^{-2}$, corresponding to 3231 and 64620 satellites deployed in the spherical surface, respectively.

probability of falling within on-service periods, and in turn decreases the resulting time-average AoI.

V. CONCLUSION

In this paper, we conducted a comprehensive analysis of the Age of Information in NTN, focusing on LEO satellite networks. By formulating an on-off process to approximate the service process between LEO satellites and a source node on Earth, we derived a closed-form expression for the time-average AoI using stochastic geometry tools. We also provided numerical results that validate the accuracy of our analysis and contribute to a deeper understanding of the factors influencing the AoI in NTN. Specifically, we quantified the impact of source status update rate and satellite constellation density on the time-average AoI. Overall, our study fills a gap in the literature by providing the first analysis of AoI in NTN and paves the way for future research in this timely field.

ACKNOWLEDGMENTS

The work of Y. Lu and H. H. Yang has been supported in part by the Zhejiang Provincial Natural Science Foundation of China under Grant LGJ22F010001 and in part by the Zhejiang Lab Open Research Project (No. K2022PD0AB05). The work of N. Pappas has been supported in part by the Swedish Research Council (VR), ELLIIT, Zenith, and the European Union (ETHER, 101096526). The work of G. Geraci was supported in part by the Spanish Research Agency through grants PID2021-123999OB-I00 and CEX2021-001195-M, by the UPF-Fractus Chair, and by the Spanish Ministry of Economic Affairs and Digital Transformation and the European Union through grants TSI-063000-2021-59 (RISC-6G), TSI-063000-2021-138 (6G-SORUS), and TSI-063000-2021-52 (AEON-ZERO).

REFERENCES

[1] X. Lin *et al.*, “5G from space: An overview of 3GPP non-terrestrial networks,” *IEEE Commun. Standards Mag.*, vol. 5, no. 4, pp. 147–153, Dec. 2021.

[2] M. Giordani and M. Zorzi, “Non-terrestrial networks in the 6G era: Challenges and opportunities,” *IEEE Network*, vol. 35, no. 2, pp. 244–251, Apr. 2021.

[3] X. Lin *et al.*, “On the path to 6G: Embracing the next wave of low Earth orbit satellite access,” *IEEE Commun. Mag.*, vol. 59, no. 12, pp. 36–42, Dec. 2021.

[4] G. Geraci *et al.*, “What will the future of UAV cellular communications be? A flight from 5G to 6G,” *IEEE Commun. Surveys Tuts.*, vol. 24, no. 3, pp. 1304–1335, 2022.

[5] E. Oughton *et al.*, “Prospective evaluation of next generation wireless broadband technologies: 6G versus Wi-Fi 7/8,” Available at SSRN: <https://ssrn.com/abstract=4528119>, 2023.

[6] G. Geraci *et al.*, “Integrating terrestrial and non-terrestrial networks: 3D opportunities and challenges,” *IEEE Commun. Mag.*, pp. 1–7, Apr. 2023.

[7] F. Wang *et al.*, “Optimizing cache content placement in integrated terrestrial and non-terrestrial networks,” in *Proc. IEEE Globecom*, 2023, pp. 1–6.

[8] M. Benzaghta *et al.*, “UAV communications in integrated terrestrial and non-terrestrial networks,” in *Proc. IEEE Globecom*, 2022, pp. 1–6.

[9] I. Leyva-Mayorga *et al.*, “NGSO constellation design for global connectivity,” *arXiv:2203.16597*, 2022.

[10] T. Darwish *et al.*, “LEO satellites in 5G and beyond networks: A review from a standardization perspective,” *IEEE Access*, vol. 10, pp. 35 040–35 060, Mar. 2022.

[11] B. Al Homssi *et al.*, “Next generation mega satellite networks for access equality: Opportunities, challenges, and performance,” *IEEE Commun. Mag.*, vol. 60, no. 4, pp. 18–24, Apr. 2022.

[12] O. Kodheli *et al.*, “Satellite communications in the new space era: A survey and future challenges,” *IEEE Commun. Surveys Tuts.*, vol. 23, no. 1, pp. 70–109, 2021.

[13] I. Del Portillo *et al.*, “A technical comparison of three low earth orbit satellite constellation systems to provide global broadband,” *Acta Astronaut.*, vol. 159, pp. 123–135, Jun. 2019.

[14] Y. Sun *et al.*, *Age of Information: A New Metric for Information Freshness*. Morgan & Claypool Publishers, 2019.

[15] N. Pappas *et al.*, *Age of Information: Foundations and Applications*. Cambridge University Press, 2023.

[16] I. Kadota *et al.*, “Optimizing age of information in wireless networks with throughput constraints,” in *IEEE INFOCOM 2018-IEEE Conference on Computer Communications*. IEEE, 2018, pp. 1844–1852.

[17] R. D. Yates *et al.*, “Age of information: An introduction and survey,” *IEEE J. Sel. Areas Commun.*, vol. 39, no. 5, pp. 1183–1210, May 2021.

[18] D.-H. Jung *et al.*, “Performance analysis of satellite communication system under the shadowed-rician fading: A stochastic geometry approach,” *IEEE Trans Commun*, vol. 70, no. 4, pp. 2707–2721, Apr. 2022.

[19] A. Talgat *et al.*, “Stochastic geometry-based analysis of leo satellite communication systems,” *IEEE Commun. Lett.*, vol. 25, no. 8, pp. 2458–2462, Aug. 2021.

[20] —, “Nearest neighbor and contact distance distribution for binomial point process on spherical surfaces,” *IEEE Commun. Lett.*, vol. 24, no. 12, pp. 2659–2663, Dec. 2020.

[21] A. Al-Hourani, “An analytic approach for modeling the coverage performance of dense satellite networks,” *IEEE Wireless Commun. Lett.*, vol. 10, no. 4, pp. 897–901, Apr. 2021.

[22] N. Okati *et al.*, “Downlink coverage and rate analysis of low earth orbit satellite constellations using stochastic geometry,” *IEEE Trans Commun*, vol. 68, no. 8, pp. 5120–5134, Aug. 2020.

[23] A. Sinha *et al.*, “Age of information with on-off service,” *IEEE Information Theory Workshop (ITW)*, 2023.

[24] A. Al-Hourani, “Optimal satellite constellation altitude for maximal coverage,” *IEEE Wireless Commun. Lett.*, vol. 10, no. 7, pp. 1444–1448, Jul. 2021.

[25] J. Park *et al.*, “A tractable approach to coverage analysis in downlink satellite networks,” *IEEE Trans. Wirel. Commun.*, Feb. 2023.

[26] P. Madadi *et al.*, “Shared rate process for mobile users in poisson networks and applications,” *IEEE Trans. Inf. Theory*, vol. 64, no. 3, pp. 2121–2141, Mar. 2018.

[27] FCC, “SpaceX non-geostationary satellite system (2018),” available online at <https://fcc.report/IBFS/SAT-MOD-20181108-00083/1569860>.

[28] Wikipedia, “Starlink,” available online at <https://en.wikipedia.org/wiki/Starlink>.

[29] —, “OneWeb,” available online at <https://en.wikipedia.org/wiki/OneWeb>.